Published in final edited form as:
Astrobiology. 2017 August ; 17(8): 761–770. doi:10.1089/ast.2016.1613.

The Formation of Nucleobases from the Ultraviolet Photo-Irradiation of Purine in Simple Astrophysical Ice Analogs

Christopher K. Materese[1,2], **Michel Nuevo**[1,2], and **Scott A. Sandford**[1,*]

[1]NASA Ames Research Center, Space Science and Astrobiology Division, MS 245-6, Moffett Field, CA 94035, USA

[2]Bay Area Environmental Research Institute, 625 2nd St., Suite 209, Petaluma, CA 94952, USA

Abstract

Nucleobases are the informational subunits of RNA and DNA and are essential to all known forms of life. The nucleobases can be divided into two groups of molecules: the pyrimidine-based compounds that include uracil, cytosine, and thymine, and the purine-based compounds that include adenine and guanine. Previous work in our laboratory has demonstrated that uracil, cytosine, thymine and other non-biological, less common nucleobases can form abiotically from the ultraviolet (UV) photo-irradiation of pyrimidine in simple astrophysical ice analogs containing combinations of H_2O, NH_3, and CH_4. In this work, we focused on the UV photo-irradiation of purine mixed with combinations of H_2O and NH_3 ices to determine whether or not the full complement of biological nucleobases can be formed abiotically under astrophysical conditions. Room temperature analyses of the resulting photoproducts resulted in the detection of adenine, guanine, and numerous other functionalized purine derivatives.

Keywords

Pyrimidine — Nucleobases — Interstellar; Ices — Cometary; Ices — Molecular processes — Prebiotic chemistry

1. Introduction

Nucleobases play an important role in life on Earth, and their function as genetic information storage constitutes a major event in the evolution of biological organisms. RNA and DNA polymers consist of a sugar and phosphate backbone with the genetic information encoded by nucleobases covalently bonded to each sugar. In the early stages of the evolution of life, RNA specifically may have served as both a functional catalyst and information-bearing molecule that permitted early cells to reproduce themselves. Because of their potential involvement in the emergence of life, understanding the abiotic formation of nucleobases is of great interest.

Biological nucleobases fall into two main families: pyrimidines (uracil, cytosine, and thymine) and purines (adenine and guanine). All of these belong to a class of molecules

[*]*Corresponding author:* Scott A. Sandford, Scott.A.Sandford@nasa.gov, Phone: (+1) 650 604 6849, Fax: (+1) 650 604 6779.

known as nitrogen heterocycles (*N*-heterocycles). *N*-heterocycles are aromatic molecules with one or more nitrogen atoms incorporated into their aromatic ring(s). Many *N*-heterocycles, including nucleobases, have been detected in carbonaceous chondrites such as Murchison, Murray, Orgueil, Allan Hills 83100, Lewis Cliff 90500, and Lonewolf Nunataks 94102 (Folsome et al. 1971; Hayatsu et al. 1975; Stoks & Schwartz 1979; Callahan et al. 2011), and the extraterrestrial origins of some of these compounds have been suggested by isotopic measurements (Martins et al. 2008). It is possible that *N*-heterocycles are produced in interstellar environments along with polycyclic aromatic hydrocarbons (PAH), in the outflows of late-type carbon (AGB) stars. In these environments, acetylene polymerization can lead to the production of PAHs (e.g., Cherchneff et al. 1992). If HCN is also present, it can substitute for one or more acetylene molecules during the polymerization process, resulting in the formation of *N*-heterocycles (Frenklach and Feigelson 1989; Ricca et al. 2001; Hamid et al. 2014). Despite the plausibility of their formation, to date no small aromatic *N*-heterocycles have been unambiguously observed in the gas phase in space (Simon and Simon 1973; Kuan et al. 2004; Charnley et al. 2005; Brünken et al. 2006).

In cold astrophysical environments, such as the interiors of dense molecular clouds and portions of protostellar disks, many gas-phase species, including PAHs, condense onto dust grains and form icy mantles. These icy mantles are subjected to ionizing radiation from various internal and external sources (e.g., UV and particle radiation from stars contained within the cloud, or external sources such as galactic cosmic rays). Laboratory experiments have sought to model these conditions using cryo-vacuum chambers equipped with a source of ionizing radiation (typically UV photons or energetic particles). These experiments have demonstrated that despite the low temperatures, radiation chemistry often leads to the production of new, more complex species (Allamandola et al. 1988; Bernstein et al. 1995; Moore and Hudson 1998; Gerakines et al 2001; Meierhenrich et al. 2005; Bennett and Kaiser 2007; Callahan et al. 2013). Following similar protocols, recent laboratory experiments have demonstrated that the UV photoprocessing of the small aromatic hydrocarbons benzene and naphthalene in combinations of H_2O and NH_3 ice mixtures results in the production of small *N*-heterocycles (Materese et al. 2015).

Radiation-induced ice chemistry is driven by the production of ions and radicals that may react with their neighbors in the surrounding ice matrix. Because the ice forms a solid matrix at very low temperatures, mobility is limited for all but the smallest ions and radicals, and those that are unable to react with their neighbors may remain trapped. Disruptions in the matrix caused by events such as a change in temperature or the absorption of a UV photon may provide new opportunities for reactions; consequently, many products are not formed until the ice is warmed. These reactions can be characterized as a chemistry of opportunity (Sandford et al. 2015) and can lead to products that are kinetically favorable rather the most energetically favorable. Often, the products of these reactions form refractory organic residues that are stable at much higher temperatures (>273 K) (Hagen et al. 1979; Allamandola et al. 1988; Bernstein et al. 1995).

Computer modeling has demonstrated that icy grains in a protosolar nebula can migrate from extremely cold regions in the outer disk or disk midplane where they can accumulate icy mantles, to warmer, less dense regions where the condensed ices may be exposed to high

energy radiation, undergo phase changes, or sublime, driving further chemistry (Ciesla and Sandford 2012). This implies that dust grains may undergo numerous cycles during which icy mantles are alternatively condensed, irradiated, and shed, thereby resulting in the formation of complex organic coatings. Eventually, these grains and their organic coatings may become incorporated into larger parent bodies such as asteroids or comets, so that any complex organic compounds produced from prior ice irradiation may be delivered to planets via meteorites or interplanetary dust particles (IDPs).

In an effort to gain insight into the origin of extraterrestrial nucleobases, extensive work was performed in our laboratory to study the photochemistry of pyrimidine in both simple and realistic astrophysical ices (Nuevo et al. 2009, 2012, 2014; Materese et al. 2013). We demonstrated that the UV photoprocessing of pyrimidine in H_2O-rich ice mixtures that contain NH_3 or CH_4 leads to the formation of the nucleobases uracil, cytosine, and thymine (Nuevo et al. 2009, 2012; Materese et al. 2013). Of these, thymine was by far the least efficiently produced nucleobase, probably because it requires more alterations from the initial pyrimidine than either uracil or cytosine, and because $–CH_3$ addition was shown to be less energetically favorable than –OH and $–NH_2$ additions (Materese et al. 2013; Sandford et al. 2015; Bera et al. 2016a).

In this work, we build upon our effort to understand the origin of nucleobases by studying the photochemistry of purine in simple astrophysical ices to examine whether the remaining nucleobases adenine and guanine, and related compounds, can be formed in a similar fashion. Additionally, a companion theoretical work examining the chemistry of this purine photochemistry has been completed (Bera et al. 2016b).

2. Experimental Methods

Pre-mixed gases (H_2O, NH_3, or H_2O+NH_3) stored in glass sample bulbs were simultaneously deposited with low-volatility purine onto an aluminum foil substrate attached to a cryo-cooled cold finger mounted inside a vacuum chamber. The vacuum chamber operates with a background pressure of $2–5\times10^{-8}$ mbar at low temperature. The residual pressure in the system is mostly due to H_2O vapor. The substrate (Al foil) upon which samples are deposited were pre-baked in air overnight at a temperature of 500°C to remove contaminant organics and mounted on the sample head of a closed-cycle helium cryo-cooler that typically operates at ~15 K.

Sample preparation was carried out using well-established experimental procedures that have been used in the NASA Ames Astrochemistry Laboratory (e.g., Allamandola et al. 1988; Bernstein et al. 1995; Bernstein et al. 1999; Nuevo et al. 2009, 2012, 2014; Materese et al. 2013, 2015). In a typical experiment, 2-liter glass bulbs were filled with H_2O vapor, NH_3 gas, or a mixture of H_2O vapor and NH_3 gas using a glass manifold. This manifold operates with background pressures of approximately 5×10^{-6} mbar, while sample bulbs were prepared with pressures between 18 to 25 mbar of sample gas. The relative abundances of the gaseous components in the starting mixture were determined by their partial pressure with an accuracy of 0.05 mbar. The following compounds were used in these experiments: H_2O (liquid; purified to 18.2 MΩ cm by a Millipore Direct-Q UV 3 device, and freeze-

pump-thawed three times to remove excess dissolved gases), NH_3 (gas; Matheson, anhydrous, 99.99%), $H_2{}^{18}O$ (liquid; Cambridge Isotope Laboratory, 97% ^{18}O, freeze-pump-thawed three times to remove excess dissolved gases), and $^{15}NH_3$ (gas; Cambridge Isotope Laboratory, 98% ^{15}N).

Since purine has an extremely low vapor pressure at room temperature, its vapor could not be mixed with H_2O vapor and/or NH_3 gas in the initial sample bulbs. Instead, a glass tube fitted with resistive heaters was prepared to allow for the simultaneous deposition of purine and the more volatile ice components. The deposition rate of purine (solid; Sigma-Aldrich, 98%, cooled and pumped three times to remove excess adsorbed gases) was calibrated by independent experiments in which the sample tube was warmed and held at a constant temperature while the purine was deposited onto the cooled substrate for 3 and 6 hours. After deposition, the amount of purine deposited was determined by extracting the purine from the foil with dimethylformamide (DMF; Thermo, silylation grade) and by analyzing the solution with gas chromatography coupled with mass spectroscopy (GC-MS), using the same protocol for the samples and standards (see below). The peak intensity for the sample was calibrated against a purine standard of known concentration and the deposition rate was assumed to be constant throughout the 3- and 6-hour experiments. The tube containing purine was heated to 70°C, which provided a deposition rate of purine of 4.3×10^{-8} mol hr^{-1}.

Simultaneous deposition of the purine and sample gases resulted in the following ice sample mixtures: H_2O:purine experiments had relative proportions of $1.0{:}10^{-3}$, H_2O:NH_3:purine experiments had relative proportions of $1.0{:}0.1{:}10^{-3}$, and NH_3:purine experiments had relative proportions of $1.0{:}10^{-3}$.

The deposition for a typical experiment lasted 44−48 hr. During deposition, the ice and purine were simultaneously irradiated with UV photons produced from a microwave-powered H_2 UV lamp. This lamp emits Lyman-α photons (121.6 nm) and a continuum centered around 160 nm with an estimated total flux ~10^{15} photons cm^{-2} s^{-1} (Warnek 1962). This lamp, chosen to simulate the UV radiation field from nearby stars and protostars in astrophysical environments, produces UV photons at a steady flux, so that the total radiation dose received by a sample is controlled by varying the irradiation time and deposition rate of the ices. The total photon doses for typical experiments are equivalent to about ~10^4 years in the diffuse interstellar medium (ISM) and ~10^7–10^9 years in the dense ISM (Mathis et al. 1983; Prasad & Tarafdar 1983; Shen et al. 2004). These dosage time equivalents for the dense ISM are only approximate, and our laboratory doses likely correspond to much shorter timescales for the irradiation of ices migrating in protoplanetary disks (Ciesla and Sandford 2012).

After deposition and irradiation, samples were slowly warmed to room temperature and then removed from the vacuum system. We note that although significant chemistry may occur during the warming phases of laboratory experiments, this process mimics the warming events that occur on grains as they warmed by nearby stars in dense interstellar clouds or move within the solar nebula (Ciesla and Sandford 2012).

In preparation for GC-MS analysis, the materials recovered on the foils were directly extracted with 25 μL of DMF (Thermo, silylation grade) and 75 μL of *N,O*-bis(trimethylsilyl) trifuoroacetamide (BSTFA) with 1% trimethylchlorosilane (Restek) and transferred to pre-baked vials (500°C). The extracts were then heated to 80°C for 1 hr to convert functionalized hydrogen moieties such as OH, NH, and NH_2 into their trimethylsilyl (TMS) derivatives.

Separation was carried out with a Thermo Trace gas chromatograph equipped with an Agilent DB-17HT column (length: 30 m, inner diameter: 0.25 mm, film thickness: 0.15 μm), coupled to a DSQ II mass spectrometer. A 1-μL aliquot of each sample or standard was injected with a splitless injection and an injector temperature of 250°C into a helium (carrier gas; Madco, ultra pure research grade, 99.99% purity) flow of 1.3 mL min^{-1}. Initially, the column temperature was held at 100°C for 2 min, and was then ramped up by 10°C min^{-1} until it reached a final temperature of 300°C, which was then held for 5 min. Masses were recorded between 50 and 550 Da (daltons), and data analysis was performed using the Xcalibur™ software (Thermo Finnigan). Peaks in the sample chromatograms were identified and quantified by comparison of both the retention times and mass spectra of the chromatographic peaks obtained for standards of known concentration derivatized using to the same protocol as the samples. Research grade standards searched for in our samples include 2-aminopurine (nitrate salt; Sigma), adenine (Sigma), hypoxanthine (Aldrich), guanine (TCI), isoguanine (TCI), 2,6-diaminopurine (Aldrich), and xanthine (California Corporation for Biochemical Research).

3. Results

Identification of compounds by GC-MS was performed by comparing single-ion chromatograms (SICs) of our samples with standards for the mass M^* (in Da) of the most intense fragment of their TMS derivatives, i.e., $M^* = M + n \times 72$, where M is the mass of the base compound (before TMS derivatization) and n is the number of TMS groups that replace functionalized hydrogens. When a peak in the chromatogram of our sample was found to match the retention time of one of our standards, the full mass spectra of each were compared for verification. As an additional degree of confirmation, some experiments were repeated using ^{18}O-labeled H_2O and ^{15}N-labeled NH_3 in the starting mixtures to ensure that the masses of the identified photoproducts were shifted as expected based on the previous identifications with unlabeled H_2O and NH_3.

For brevity, we have only included the chromatograms and corresponding mass spectra for hypoxanthine, adenine, and guanine here. The chromatograms and corresponding mass spectra for all other identified compounds can be found in the supplementary materials. All identified compounds are listed in Table 1 along with their formulae, molecular masses, retention times (R_t), masses of their TMS derivatives in the GC-MS chromatograms (M^*), and their abundances. Abundances reported in Table 1 were obtained from one typical experiment with H_2O:NH_3:purine ($1.0:0.1:10^{-3}$) ice mixtures, by integrating peaks in the sample chromatogram and comparing them to reference standards of known concentration. The concentration of the unaltered purine remaining in our samples could not be determined using this method because its peak was usually saturated. Note that all chromatograms

shown here have been rescaled for visual simplicity so that the magnitudes of the largest visible peaks are the same height for the samples and standards. In addition, for ease of comparison, each mass spectra was rescaled to the most abundant mass fragment. (Note that mass 73, which corresponds to the TMS $[(CH_3)_3Si]^+$ ion fragment and that is present in all the mass spectra, has been excluded from setting the scale.)

3.1. H_2O:purine mixtures

Our initial experiments involved the UV photoprocessing of H_2O ice containing purine in a ratio of $1.0:10^{-3}$. This resulted in the production of numerous oxidized photoproducts including hypoxanthine (Fig. 1) and xanthine (Fig. S1). Two unidentified peaks were also observed (R_t = 11.42 and 12.34 min) with mass spectra consistent with purine bearing one OH moiety (i.e., isomers of hypoxanthine). Additionally, two unidentified peaks were observed (12.49 and 13.77 min) with mass spectra consistent with purine bearing two OH moieties (i.e., isomers of xanthine). There were no readily available standards that could be purchased to confirm the identity of these additional isomers; however, the mass spectra of these compounds possess strong similarities to hypoxanthine and xanthine, respectively, suggesting that they are most likely purines with either one or two OH moieties added to peripheral carbon positions that are different from those in hypoxanthine and xanthine. This suggests that OH moieties can replace any of the hydrogens bound to carbon atoms in the purine molecule (Fig. 2). It should be noted that no *N*-oxides were detected in these samples.

3.2. NH_3:purine mixtures

Experiments involving the UV photoprocessing of NH_3 ices containing purine in $1.0:10^{-3}$ ratios did not produce detectable levels of any photoproducts with the exception of trace quantities of adenine (Table 1, see Section 3.3 and Fig. 3 for the chromatogram and mass spectrum of this compound). These results are similar to our previous work with pyrimidine, in which very few photoproducts were observed in the absence of any H_2O in the starting sample ice matrix (Nuevo et al. 2012).

3.3. H_2O:NH_3:purine mixtures

Experiments involving the UV photoprocessing of H_2O:NH_3:purine ices (relative abundances of $1.0:0.1:10^{-3}$) resulted in the production of numerous photoproducts including hypoxanthine (Fig. 1), xanthine (Fig. S1), adenine (Fig. 3), 2-aminopurine (Fig. S2), 2,6-diaminopurine (Fig. S3), isoguanine (Fig. S4), and guanine (Fig. 4). The same unidentified peaks as seen in the H_2O:purine experiments were also observed in these residues and likely belong to singly and doubly oxidized purines. Two new unidentified peaks were observed (R_t = 11.92 and 13.18 min), with mass spectra consistent with purine bearing two NH_2 moieties. Similarly to what was seen with the addition of OH moieties, this suggests that –NH_2 can also replace any of the hydrogens bound to carbon atoms in the purine molecule (Fig. 5). Additionally, two unidentified peaks were observed (R_t = 13.09 and 14.45 min) with mass spectra consistent with purine bearing exactly one NH_2 and one OH moiety (i.e., isomers of guanine and isoguanine).

To further confirm our identifications and to support our hypotheses for the characterization of the unidentified peaks, we repeated these experiments with ^{18}O-labeled water and ^{15}N-

labeled ammonia in the starting ice mixtures, the results of which are shown in the mass spectra provided in Figs. 1, 3, and 4, in addition to supplementary Figs. S1−S3. Each ^{18}O added to purine is 2 Da heavier compared with each ^{16}O from regular H_2O (e.g., the parent peaks of hypoxanthine and xanthine shift from 280 to 282 Da and from 368 to 372 Da, respectively). Likewise, each ^{15}N added to purine is 1 Da heavier compared with each ^{14}N from regular NH_3 (e.g., the parent peak of adenine shifts from 279 to 280 Da). In each case, we find that the mass spectra of all of the identified and hypothesized isomeric photoproducts shift as expected, improving confidence in the identification of these molecules, and supporting the hypothesis that the unidentified peaks are due to the presence of isomers with the relevant number of added OH and/or NH_2 moieties.

4. Discussion

4.1. Competition between OH and NH_2 addition

Our experiments indicate that both OH and NH_2 moieties can readily replace any of the hydrogens bound to carbon atoms in the original purine. This result is supported by the fact that our samples appear to contain all isomers of both singly OH- and NH_2-substituted purine compounds. While we cannot determine differences in the relative abundances of each isomer with any certainty, given that standards are not commercially available for all the isomers in question, our results allow us to directly compare the relative abundances of OH vs. NH_2 substitutions at position 6 between hypoxanthine and adenine. We note that the residue whose chromatograms are shown in Figs. 1, 3, and 4 contains 120 nmol of hypoxanthine and 31 nmol of adenine (Table 1), i.e., relative abundances of about 4:1. However, as the initial ice contained 10 H_2O molecules for every NH_3 molecule, this suggests that NH_2 addition to purine is 2.5 times more efficient at this position than OH addition. Additionally, we note that this residue contains 0.58 nmol of isoguanine, 0.25 nmol of guanine, and 0.11 nmol of 2,6-diaminopurine (i.e., relative abundances of isoguanine:2,6-diaminopurine ~ 5:1 and guanine:2,6-diaminopurine ~ 2.5:1). A similar observation can be made by comparing the relative abundances of hypoxanthine to 2-aminopurine although the position of the substitution is no longer the same. These findings suggest that the replacement of peripheral hydrogens in purine by an NH_2 group is slightly favored over an OH group for the isomers for which we have standards. This result differs somewhat from our previous experiments involving the photoprocessing of pyrimidine containing astrophysical ice analogs (Nuevo et al. 2014). In that work, the relative abundances of OH- and NH_2-bearing photoproducts were proportional to the relative abundances of H_2O and NH_3 in the initial gas mixture. We note that this observation is limited only to the directly comparable case of hypoxanthine versus adenine formation and does not necessarily extend to other substitutions.

4.2. Comparison with meteorites

Our experiments are designed to simulate the conditions of dense molecular clouds and the early protosolar nebula using reactants that are simplified analogs of the icy mantles that are observed on astrophysical dust grains. Consequently, the resulting residues produced in our experiments can be considered to be analogous to the primitive dusty materials that aggregated in the protosolar nebula and that were ultimately incorporated into comets and

asteroids. Some of these materials, and their alteration products, were then subsequently delivered to telluric planets in the form of cosmic dust and meteorites. It should be noted that the organic materials found in meteorites have often undergone significant asteroidal parent body processing in the form of aqueous alteration and heating that likely altered their original, pre-solar nebula composition. Nonetheless, it is useful to compare our experimental results to the materials detected in meteorites to look for similarities and differences.

Numerous efforts have been made to characterize and quantify the purines in meteorites (Hayatsu 1964; Hayatsu et al. 1975; Van der Velden and Schwartz 1977; Callahan et al. 2011). The most recent and extensive effort was completed by Callahan et al. (2011) and involved samples from a dozen meteorites that show different levels of aqueous alteration. Purines reported in these meteorites include guanine, hypoxanthine, xanthine, adenine, 2,6-diaminopurine, and 6,8-diaminopurine. With the exception of 6,8-diaminopurine, for which we could not find a commercial standard, all of these compounds were identified in our experimental residues. Overall, the list of nucleobases detected in our residues closely matches the list of nucleobases found in meteoritic samples. Only 2-aminopurine and isoguanine, both of which were found in our residues, were sought by Callahan et al. (2011) but not detected in any meteoritic samples. While the general suite of compounds is similar between our samples and meteorites, the relative abundances of the different compounds are frequently rather different. For example, according to Callahan et al. (2011), guanine is often the most abundant nucleobase found in meteorites, whereas the singly substituted photoproducts hypoxanthine, adenine, and 2-aminopurine are orders of magnitude more abundant than guanine in our residues.

The differences between what is detected in meteorites and our ice photoprocessing experiments can be attributed to several factors. First, our simulations are more representative of the primitive organic compound that may exist on cosmic dust grains at the time that they are incorporated into larger parent bodies. This means that the materials generated in these experiments represent materials that have not been subjected to the same parent body processes (aqueous alteration and thermal process) that may have been experienced by meteoritic samples. Second, there could be other competing processes that contribute to the production (or destruction) of nucleobases associated with aqueous alteration occurring in the meteorite parent bodies. In a very general sense, the favored products in our experiments are the products that require the fewest number of substitutions, as might be expected for this kind of chemical processes. However, if nucleobases are also formed through some parallel process(es), like parent body aqueous alteration, other products (e.g., guanine) may be favored. Finally, the detection of nucleobases in meteoritic samples requires a formic acid extraction to separate the nucleobases from other meteoritic materials. This may favor extraction of some compounds over others and change the inferred relative abundances between the identified compounds.

Although the relative abundances of the nucleobases detected in our experiments do not appear to mimic their meteoritic abundances, it is possible that they are closer to what might have been delivered to the early Earth from comets via IDPs, in which organics have probably not been subjected to aqueous alteration. However, such complex organics have not yet been searched for or identified in such small particles.

4.3. Astrobiological implications

These experiments, combined with our previous work (Nuevo et al. 2009, 2012, 2014; Materese et al. 2013), demonstrate that it is possible to abiotically produce all the nucleobases necessary for the development of DNA and RNA, if purine and pyrimidine are present in astrophysical environments and subjected to ionizing radiation. Thus, the nucleobases can be added to a growing list of compounds of astrobiological interest, including amino acids, quinones, and amphiphiles (Bernstein et al. 1999, 2002a, 2002b; Dworkin et al. 2001; Muñoz Caro et al. 2002; Nuevo et al. 2008, 2009, 2012; Materese et al. 2013) that can be made via the irradiation of ices and that were likely delivered to the early Earth, where they could have played an important role in the emergence of life.

In the experiments described in the present work, as well as the previous work related to the formation of pyrimidine-based nucleobases (Nuevo et al. 2009, 2012, 2014; Materese et al. 2013), the relative abundances of each nucleobase appears to be primarily governed by three factors: 1) the number of functional group additions required to form the product; 2) the type of functional group being added; and 3) the position where this addition takes place.

The number of functional group additions required to form a given product is important, because, generally, the abundance of a photoproduct requiring one substitution is significantly higher than the abundance of photoproducts requiring two or more substitutions. This is caused by a combination of the facts that: (i) more additions require a higher number of photons, and (ii) additional photons not only produce new photoproducts, but they can also destroy previously formed products.

The type of functional group being added is also important because some reactions are more thermodynamically favorable than others (e.g. OH or NH_2 relative to CH_3) (Bera et al. 2016a), and because the relative availability of the parent molecules of the functional groups in the surrounding ices is different for different groups. This is exemplified in this work, where we see that the addition of NH_2 groups appears to be more favorable than the addition of OH groups. However, the total abundance of OH-substituted photoproducts is still higher overall because there is more H_2O in our starting ice mixtures than there is NH_3, as it is also the case in interstellar ices.

Finally, the position of the addition is important because of differences in bond stability, conservation or loss of the aromaticity of the molecule, and statistics of identical substitutions due to molecular symmetry. These conclusions have been demonstrated experimentally by this work and prior efforts (Nuevo et al. 2009, 2012, 2014; Materese et al. 2013) and by quantum chemical calculations (Bera et al. 2010, 2016a, 2016b).

Because of these considerations, singly substituted molecules such as hypoxanthine and adenine are more abundant in our residues than doubly substituted molecules such as guanine, by several orders of magnitude. This large divergence in relative abundances between adenine and guanine (about 120:1 in our experiments) could be potentially problematic when it comes to the emergence of life. Interestingly, hypoxanthine, which is the most abundant singly oxidized purine identified in our residues, has been suggested as a base-pairing analog for guanine in DNA and RNA (Crick 1968; Nishikura 2010; Rios and

Tor 2013; Cafferty and Hud 2015). Our results would therefore be consistent with a scenario in which hypoxanthine may have served as a substitute for guanine during the emergence of life (Crick 1968; Cafferty and Hud 2015).

It is notable that one of the perennial problems with terrestrial synthetic pathways for the formation of purines and pyrimidines is that, to date, no experimental conditions have been determined that can produce both together simultaneously. However, this is not a problem for nucleobases formed in an interstellar environment from ice photochemical processes. *N*-Heterocycles including purine and pyrimidine may be produced under astrophysical conditions, either during PAH synthesis in stellar outflows from stars that contain high levels of HCN (Frenklach and Feigelson 1989; Ricca et al. 2001; Hamid et al. 2014), or *in situ* from reactions between N-bearing species and PAHs that condensed as icy mantles on cold grains (Materese et al. 2015), or a combination of both types of processes. When condensed onto icy grains, purines, pyrimidines, and their subsequent photoproducts can be produced simultaneously, driven by similar processes, and under the same conditions. These molecules can then be delivered to telluric planets together with no need for subsequent mixing of materials made by different processes in different locations.

5. Conclusion

This work has demonstrated that the nucleobases adenine and guanine can be produced from the UV photoprocessing of simple astrophysical ice analogs. More generally, the results suggest that any H attached to a peripheral carbon of the purine molecule can be substituted by NH_2 or OH groups to form all possible isomers. In many cases, double substitution compounds can also be made.

In conjunction with our previous work involving the UV photoprocessing of pyrimidines under similar experimental conditions (Nuevo et al. 2009, 2012, 2014; Materese et al. 2013), it has been demonstrated that the five main biologically important nucleobases can be produced under the same astrophysical conditions as long as there is a source of purine or pyrimidine. All five of these nucleobases can be produced under the same conditions, albeit with different relative abundances, and can be delivered together to telluric planets. This could simplify the problem of getting them together in the same place during the early stages of RNA development in a primitive terrestrial environment.

Differences in the relative abundances of each photoproduct in our residues are governed by 1) the number of functional group additions required to form a given product; 2) the type of functional group being added; and 3) the position where this addition takes place. Specifically, increasing the number of substitutions to purine greatly reduces the abundance of a given photoproduct. Moreover, experimental results suggest that NH_2 group addition to purine appears slightly more favorable than OH addition, at least at the position 6 of the purine molecule, the only position for which we have mutually comparable standards. Finally, the position of the substitution matters because of differences in energetic favorability. In a general sense, the list of purines identified in our experiments closely mirrors the purines identified in meteoritic samples. The relative abundances of these compounds are however very different, which suggests that the population of purines

identified in meteorites that were originally formed from the UV photoprocessing of interstellar ices most likely underwent parent body alteration. In contrast, purines delivered in the form of cosmic dust (IDPs) might be much closer to what is observed in our laboratory samples, since cometary materials likely undergo far less aqueous and thermal processes.

While our results demonstrate that all the nucleobases used in modern RNA and DNA can be formed in icy astrophysical environments, the relative abundances of these nucleobases vary significantly. Our previous work demonstrated that uracil and cytosine (both of which require two substitutions to the starting pyrimidine) form far more readily than thymine. Similarly, adenine appears to form far more readily than guanine. This suggests that if nucleobases produced by these processes played a role in the emergence of life, then perhaps thymine and guanine were initially less essential, and their importance may have been a later evolutionary development. In this scenario, some alternative nucleobases may have occupied these roles during the emergence of life (e.g., uracil for thymine and hypoxanthine for guanine).

Supplementary Material

Refer to Web version on PubMed Central for supplementary material.

Acknowledgments

This material is based upon work supported by the National Aeronautics and Space Administration through the NASA Astrobiology Institute under Cooperative Agreement Notice NNH13ZDA017C issued through the Science Mission Directorate. We would also like to thank the reviewers of this manuscript for their thoughtful comments.

References

Allamandola LJ, Sandford SA, Valero GJ. Photochemical and thermal evolution of interstellar/precometary ice analogs. Icarus. 1988; 76:225–252.

Bennett CJ, Kaiser RI. On the formation of glycolaldehyde ($HCOCH_2OH$) and methyl formate ($HCOOCH_3$) in interstellar ice analogs. Astrophys J. 2007; 600:1289–1295.

Bera PP, Nuevo M, Milam SN, Sandford SA, Lee TJ. Mechanism for the abiotic synthesis of uracil via UV-induced oxidation of pyrimidine in pure H_2O ices under astrophysical conditions. J Chem Phys. 2010; 133:104303. [PubMed: 20849168]

Bera PP, Nuevo M, Materese CK, Lee TJ, Sandford SA. Mechanism for the formation of thymine under astrophysical conditions, and implications for the origin of life. J Chem Phys. 2016a; 144:144308, 7. [PubMed: 27083722]

Bera PP, Stein T, Head-Gordon M, Lee TJ. Mechanisms of the formation of adenine, guanine, and their analogs in irradiated mixed molecular ices. Astrobiology. 2016b submitted.

Bernstein MP, Sandford SA, Allamandola LJ, Chang S. Organic compounds produced by photolysis of realistic interstellar and cometary ice analogs containing methanol. Astrophys J. 1995; 454:327–344.

Bernstein MP, Sandford SA, Allamandola LJ, Gillette JS, Clemett SJ, Zare RN. UV irradiation of polycyclic aromatic hydrocarbons in ices: production of alcohols, quinones, and ethers. Science. 1999; 283:1135–1138. [PubMed: 10024233]

Bernstein MP, Dworkin JP, Sandford SA, Cooper GW, Allamandola LJ. The formation of racemic amino acids by ultraviolet photolysis of interstellar ice analogs. Nature. 2002a; 416:401–403. [PubMed: 11919623]

Bernstein MP, Elsila JE, Dworkin JP, Sandford SA, Allamandola LJ, Zare RN. Side group addition to the PAH coronene by UV photolysis in cosmic ice analogs. Astrophys J. 2002b; 576:1115–1120.

Brünken S, McCarthy MC, Thaddeus P, Godfrey PD, Brown RD. Improved line frequencies for the nucleic acid base uracil for a radioastronomical search. Astron Astrophys. 2006; 459:317–320.

Cafferty BJ, Hud NV. Was a Pyrimidine-Pyrimidine Base Pair the Ancestor of Watson-Crick Base Pairs? Insights from a Systematic Approach to the Origin of RNA. Isr J Chem. 2015; 55:891–905.

Callahan MP, Smith KE, Cleaves HJ II, Ruzicka J, Stern JC, Glavin DP, House CH, Dworkin JP. Carbonaceous meteorites contain a wide range of extraterrestrial nucleobases. Proc Natl Acad Sci. 2011; 108:13995–13998. [PubMed: 21836052]

Callahan MP, Gerakines PA, Martin MG, Peeters Z, Hudson RL. Irradiated benzene ice provides clues to meteoritic organic chemistry. Icarus. 2013; 226:1201–1209.

Charnley SB, Kuan YJ, Huang HC, Botta O, Butner HM, Cox N, Despois D, Ehrenfreund P, Kisiel Z, Lee YY, Markwick AJ, Peeters Z, Rodgers SD. Astronomical searches for nitrogen heterocycles. Adv Space Res. 2005; 36:137–145.

Cherchneff I, Barker JR, Tielens AGGM. Polycyclic aromatic hydrocarbon formation in carbon-rich stellar envelopes. Astrophys J. 1992; 401:269–287.

Ciesla FJ, Sandford SA. Organic synthesis via irradiation and warming of ice grains in the solar nebula. Science. 2012; 336:452–454. [PubMed: 22461502]

Crick FHC. The origin of genetic code. J Mol Biol. 1968; 38:367–379. [PubMed: 4887876]

Dworkin JP, Deamer DW, Sandford SA, Allamandola LJ. Self-assembling amphiphilic molecules: synthesis in simulated interstellar=precometary ices. Proc Natl Acad Sci. 2001; 98:815–819. [PubMed: 11158552]

Folsome CE, Lawless J, Romiez M, Ponnamperuma C. Heterocyclic compounds indigenous to the Murchison meteorite. Nature. 1971; 232:108–109. [PubMed: 16062864]

Frenklach M, Feigelson ED. Formation of polycyclic aromatic hydrocarbons in circumstellar envelopes. Astrophys J. 1989; 341:372–384.

Gerakines PA, Moore MH, Hudson RL. Energetic processing of laboratory ice analogs: UV photolysis versus ion bombardment. J Geophys Res. 2001; 106:33381.

Hagen W, Allamandola LJ, Greenberg M. Interstellar molecule formation in grain mantles: The laboratory analog experiments, results implications. Astrophys Space Sci. 1979; 65:215–240.

Hayatsu R. Orgueil meteorite: organic nitrogen contents. Science. 1964; 146:1291–1293. [PubMed: 17810143]

Hayatsu R, Anders E, Studier MH, Moore LP. Purines and triazines in the Murchison meteorite. Geochim Cosmochim Acta. 1975; 39:471–488.

Hamid AM, Bera PP, Lee TJ, Aziz SG, Alyoubi AO, El-Shall MS. Evidence for the formation of pyrimidine cations from the sequential reactions of hydrogen cyanide with the acetylene radical cation. J Phys Chem Lett. 2014; 5:3392–3398. [PubMed: 26278451]

Kuan YJ, Charnley SB, Huang HC, Kisiel Z, Ehrenfreund P, Tseng WL, Yan CH. Searches for interstellar molecules of potential prebiotic importance. Adv Space Res. 2004; 33:31–39.

Martins Z, Botta O, Fogel ML, Sephton MA, Glavin DP, Watson JS, Dworkin JP, Schwartz AW, Ehrenfreund P. Extraterrestrial nucleobases in the Murchison meteorite. Earth Planet Sci Let. 2008; 270:130–136.

Materese CK, Nuevo M, Bera PP, Lee TJ, Sandford SA. Thymine and other prebiotic molecules produced for the ultraviolet photo-irradiation of pyrimidine in simple astrophysical ice analogs. Astrobiology. 2013; 13:948–962. [PubMed: 24143868]

Materese CK, Nuevo M, Sandford SA. *N*- and *O*-heterocycles produced from the irradiation of benzene and naphthalene in H_2O/NH_3-containing ices. Astrophys J. 2015; 800:116–123.

Mathis JS, Mezger PG, Panagia N. Interstellar radiation field and dust temperatures in the diffuse interstellar matter and in giant molecular clouds. Astron Astrophys. 1983; 128:212–229.

Meierhenrich UJ, Muñoz Caro GM, Schutte WA, Thiemann WHP, Barbier B, Brack A. Precursors of biological cofactors from ultraviolet irradiation of circumstellar/interstellar Ice analogues. Chem Eur J. 2005; 11:4895–4900. [PubMed: 15900538]

Munoz Caro GM, Meierhenrich UJ, Schutte WA, Barbier B, Arcones Segovia A, Rosenbauer H, Thiemann WHP, Brack A, Greenberg JM. Amino acids from ultraviolet irradiation of interstellar ice analogues. Nature. 2002; 416:403–406. [PubMed: 11919624]

Moore MH, Hudson RL. Infrared study of ion-irradiated water-ice mixtures with hydrocarbons relevant to comets. Icarus. 1998; 135:518–527.

Nishikura K. Functions and Regulation of RNA Editing by ADAR deaminases. Annu Rev Biochem. 2010; 79:321–349. [PubMed: 20192758]

Nuevo M, Auger G, Blanot D, d'Hendecourt L. A detailed study of the amino acids produced from the vacuum UV irradiation of interstellar ice analogs. Orig Life Evol Biosph. 2008; 38:37–56. [PubMed: 18175206]

Nuevo M, Milam SN, Sandford SA, Elsila JE, Dworkin JP. Formation of uracil from the ultraviolet photo-irradiation of pyrimidine in pure H_2O ices. Astrobiology. 2009; 9:683–695. [PubMed: 19778279]

Nuevo M, Milam SN, Sandford SA. Nucleobases and prebiotic molecules in organic residues produced from the ultraviolet photo-irradiation of pyrimidine in NH_3 and H_2O+NH_3 ices. Astrobiology. 2012; 12:295–314. [PubMed: 22519971]

Nuevo M, Materese CK, Sandford SA. The photochemistry of pyrimidine in realistic astrophysical ices and the production of nucleobases. Astrophys J. 2014; 793:125–131.

Prasad SS, Tarafdar SP. UV radiation field inside dense clouds — Its possible existence and chemical implications. Astrophys J. 1983; 267:603–609.

Ricca A, Bauschlicher CW Jr, Bakes ELO. A computational study of the mechanisms for the incorporation of a nitrogen atom into polycyclic aromatic hydrocarbons in the Titan haze. Icarus. 2001; 154:516–521.

Rios AC, Tor Y. On the origin of the canonical nucleobases: an assessment of selection pressures across chemical and early biological evolution. Isr J Chem. 2013; 53:469–483. [PubMed: 25284884]

Sandford, SA., Bera, PP., Lee, TJ., Materese, CK., Nuevo, M. Photosynthesis and photo-stability of nucleic acids in prebiotic and extraterrestrial environments. In: Barbatti, M.Borin, AC., Ullrich, S., editors. Photoinduced Phenomena in Nucleic Acids II, Topics Curr Chem. Vol. 356. Springer; 2015. p. 123-164.

Shen CJ, Greenberg JM, Schutte WA, van Dishoeck EF. Cosmic ray induced explosive chemical desorption in dense clouds. Astron Astrophys. 2004; 415:203–215.

Simon MN, Simon M. Search for interstellar acrylonitrile, pyrimidine, and pyridine. Astrophys J. 1973; 184:757–762.

Stoks PG, Schwartz AW. Uracil in carbonaceous meteorites. Nature. 1979; 282:709–710.

Van der Velden W, Schwartz AW. Search for purines and pyrimadines in the Murchison meteorite. Geochim Cosmochim Acta. 1977; 41:961–968.

Warnek P. A microwave-powered hydrogen lamp for vacuum ultraviolet photochemical research. Appl Optics. 1962; 1:721–726.

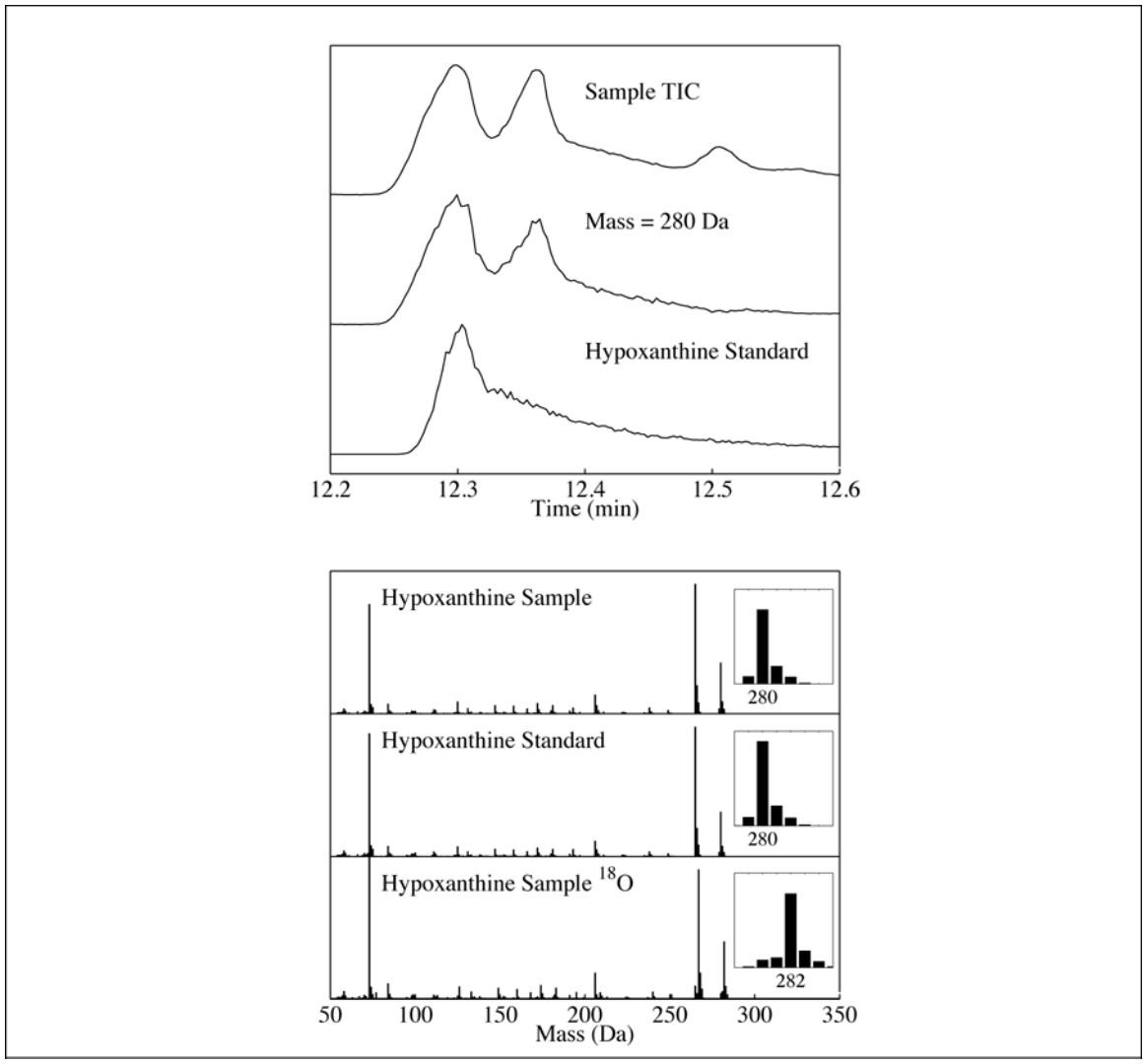

Fig 1.

Top panel: (Top Trace) Total-ion chromatogram (TIC) of the residue produced from a UV-irradiated H_2O:NH_3: purine ice. Middle trace) Single-ion chromatogram (SIC) of the same residue for mass 280 Da. (Bottom trace) SIC of the hypoxanthine standard (mass 280 Da). ***Bottom panel:*** (Top trace) Mass spectrum of the peak identified as hypoxanthine in the same residue. (Middle trace) Mass spectrum of the hypoxanthine standard. (Bottom trace) Mass spectrum of the peak identified as hypoxanthine in the residue produced from a UV-irradiated ice containing $H_2{}^{18}O$ instead of H_2O. The observed mass increase matches what is expected for the hypoxanthine identification.

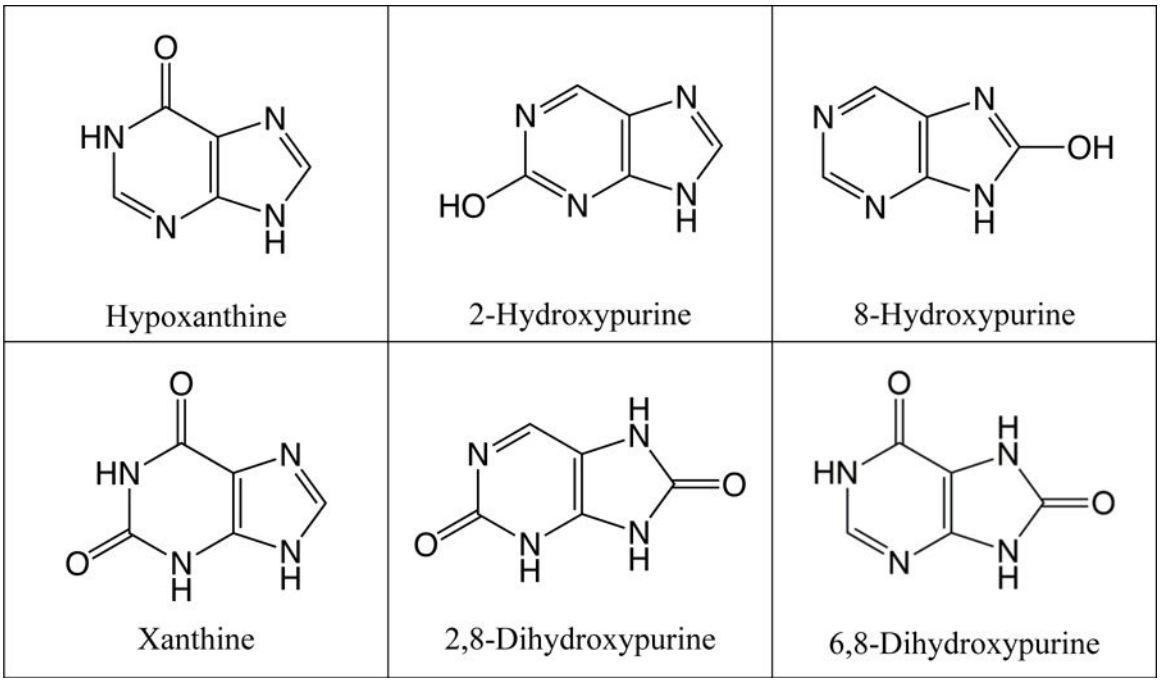

Fig. 2.

Structures of all possible singly and doubly oxidized purines (*N*-oxides excluded). The presence of hypoxanthine and xanthine have been confirmed using GC-MS by comparison with commercial standards. The remaining 4 compounds are hypothesized to also be present based on the mass spectra of several unidentified peaks in the chromatogram. However, no standards were commercially available for confirmation.

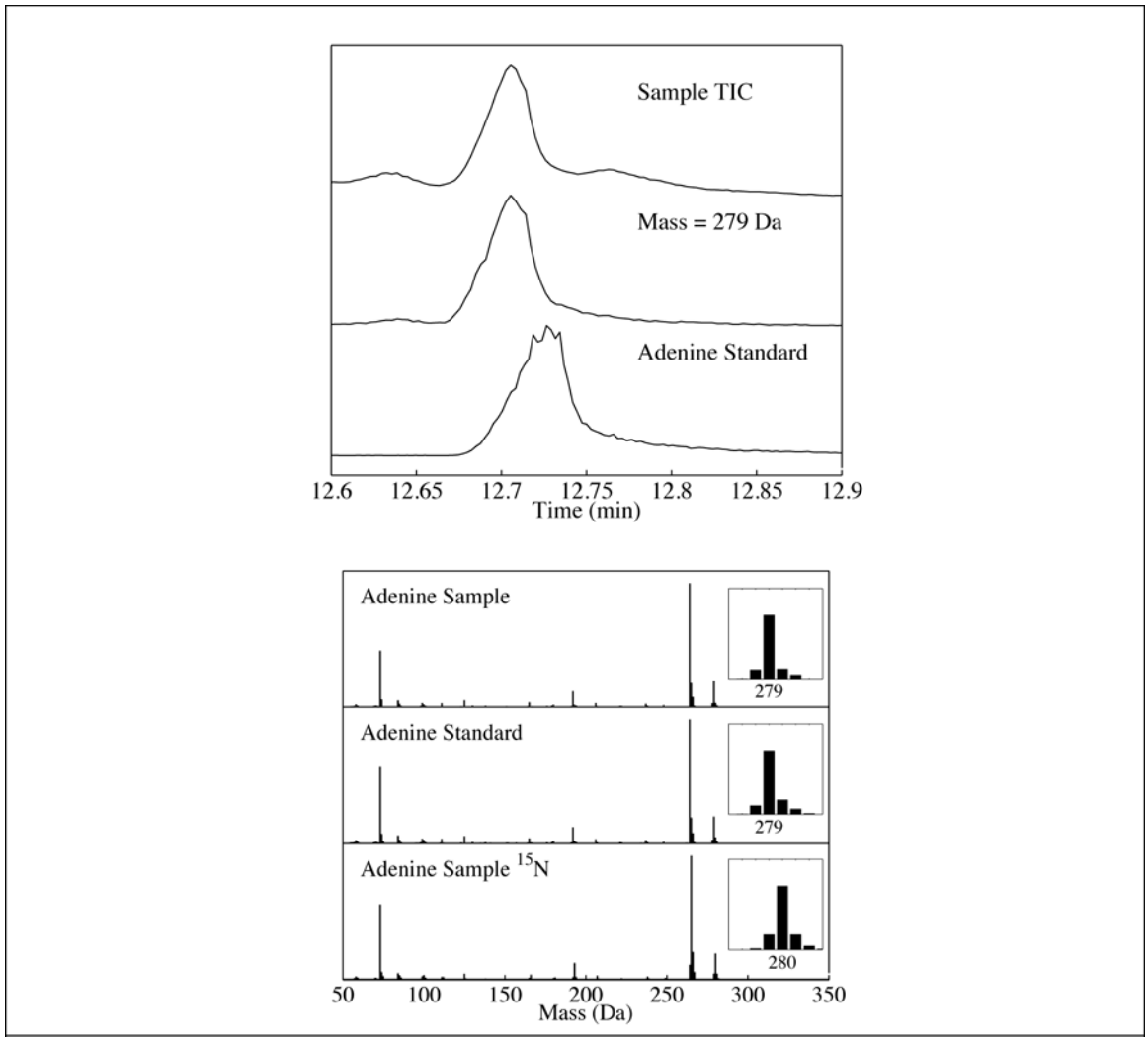

Fig 3.

Top panel: *(Top trace)* Total-ion chromatogram (TIC) of the residue produced from a UV-irradiated H_2O:NH3:purine ice. *(Middle trace)* Single-ion chromatogram (SIC) of the same residue for mass 279 Da. *(Bottom trace)* SIC of the adenine standard (mass 279 Da). ***Bottom panel:*** *(Top trace)* Mass spectrum of the peak identified as adenine in the residue produced from a UV-irradiated H_2O:NH_3:purine ice. *(Middle trace)* Mass spectrum of the adenine standard. *(Bottom trace)* Mass spectrum of the peak identified as adenine in the residue produced from a UV-irradiated ice containing $^{15}NH_3$ instead of NH_3. The observed mass increase matches what is expected for the adenine identification.

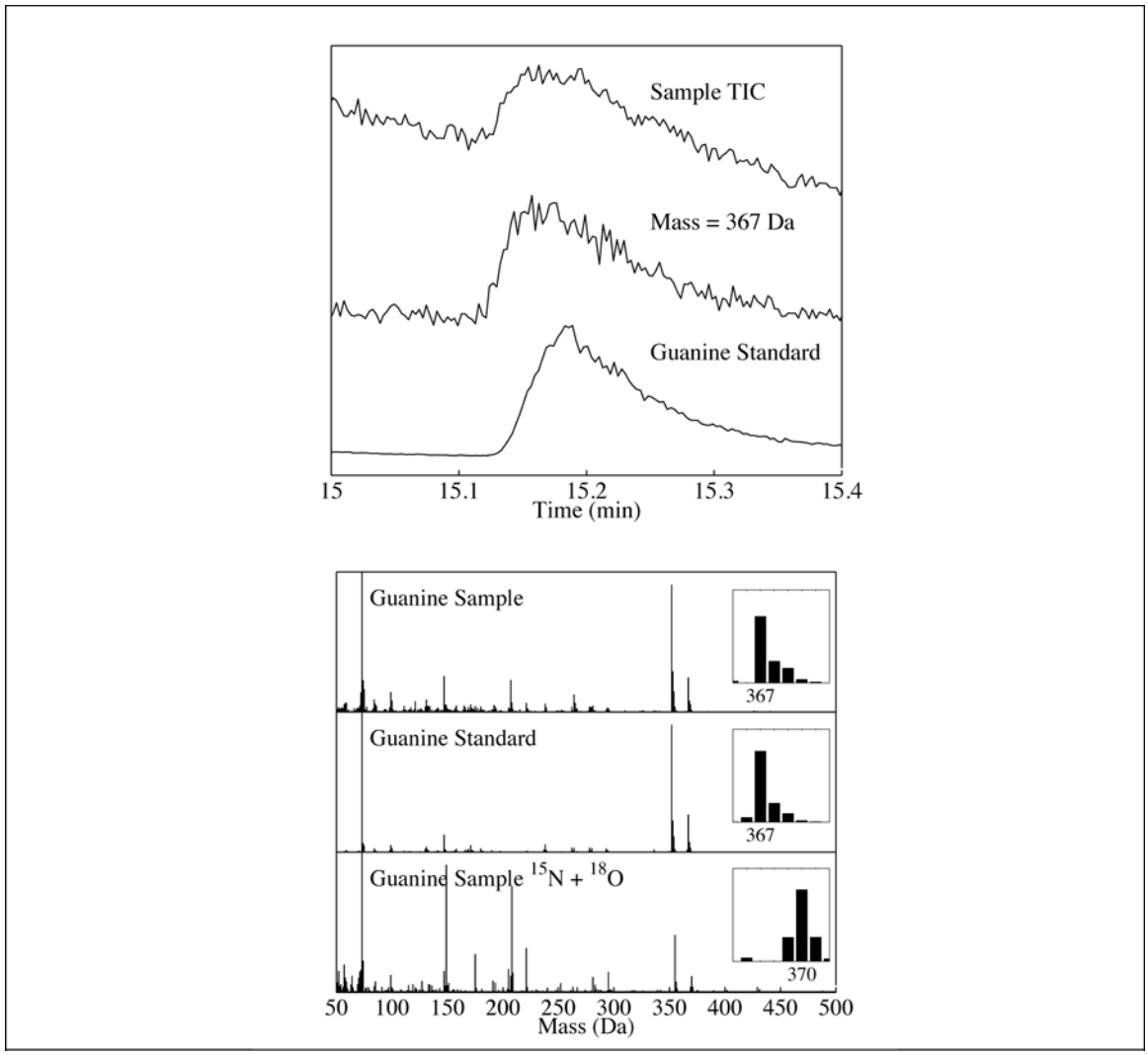

Fig 4.

Top panel: *(Top trace)* Total-ion chromatogram (TIC) of the residue produced from a UV-irradiated H2O:NH3:purine ice. *(Middle trace)* Single-ion chromatogram (SIC) of the same residue for mass 367 Da. *(Bottom trace)* SIC of the guanine standard (mass 367 Da). ***Bottom panel:*** *(Top trace)* Mass spectrum of the peak identified as guanine in the residue produced from a UV-irradiated H2O:NH3:purine ice. *(Middle trace)* Mass spectrum of a guanine standard. *(Bottom trace)* Mass spectrum of the peak identified as guanine in the residue produced from a UV-irradiated ice containing $H_2{}^{18}O$ and $^{15}NH_3$ instead of H_2O and NH_3, respectively. The observed mass increase matches what is expected for the guanine identification.

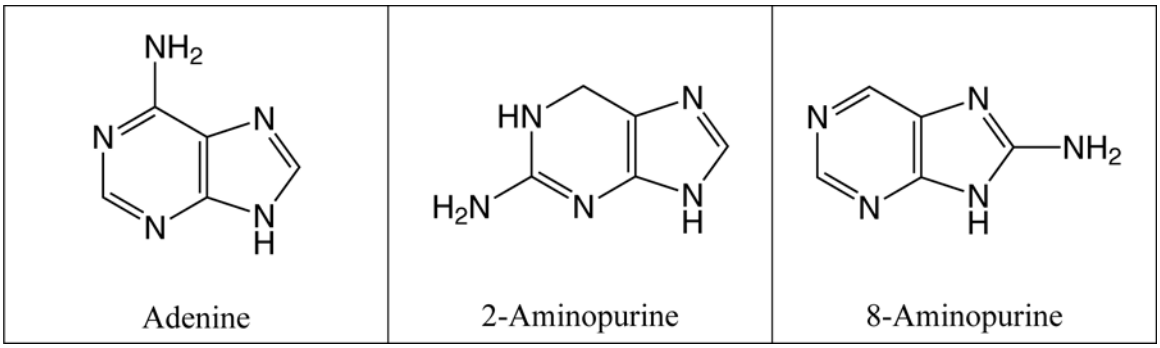

Fig. 5.

Structures of all possible singly aminated purines. The presence of adenine and 2-aminopurine have been confirmed using GC-MS by comparison with a commercial standard. 8-Aminopurine is hypothesized to also be present based on the mass spectra of several unidentified peaks in the chromatogram. However, no standards were commercially available for confirmation.

Table 1

Purine compounds identified in our residues.

Species	Formula	Molecular mass (Da)	Rt (GC-MS) (min)[a]	M* GC-MS peak (Da)[b]	Abundance in nmol (% deposited purine)
Purine	C5H4N4	120	9.31	192	–
Hypoxanthine	C5H4N4O	136	12.29	280	120 (5.7%)
Xanthine	C5H4N4O2	152	14.43	368	1.5 (0.07%)*
Adenine	C5H5N5	135	12.71	279	31 (1.5%)
2-Aminopurine	C5H5N5	135	13.20	279	42 (2.0%)
2,6-Diaminopurine	C5H6N6	150	15.46	366	0.11 (0.0052%)
Isoguanine	C5H5N5O	151	14.82	367	0.58 (0.028%)
Guanine	C5H5N5O	151	15.21	367	0.25 (0.012%)

*The abundance of xanthine could not be determined accurately because it eluted between two more abundant compounds that may be interfering with the integration. This value should be thus taken as an upper limit.